Received June 2003
Revised February 2004
Accepted February 2004

Effect of geometry on flow field and oil/water separation in vertical deadlegs

M.A. Habib, S.A.M. Said, H.M. Badr and I. Hussaini
Mechanical Engineering Department, King Fahd University of Petroleum and Minerals, Dhahran, Saudi Arabia
J.J. Al-Bagawi
Saudi Aramco, Saudi Arabia

Abstract

Purpose – Corrosion in deadlegs occurs as a result of water separation due to the very low flow velocity. The present work aims to investigate the effect of geometry on flow field oil/water separation in deadlegs in an attempt for obtaining the conditions for avoiding formation of deadleg.

Design/methodology/approach – The investigation is based on the solution of the mass and momentum conservation equations of an oil/water mixture together with the volume fraction equation for the secondary phase. A fluid flow model based on the time-averaged governing equation of 3D turbulent flow has been developed. An algebraic slip mixture model for the calculation of the two immiscible fluids (water and crude oil) is utilized.

Findings – Results are obtained for different lengths of the deadleg. The inlet flow velocity is kept unchanged (1.0 m/s) and the deadleg length to diamter ratio (L/D_B) ranges from 1 to 7. The considered fluid mixture contains 90 percent oil and 10 percent water (by volume). The results show that the size of the stagnant fluid region increases with the increase of L/D_B 1 $\approx 3D_B$.

Practical implications – Deadlegs should be avoided whenever possible in design of piping for fluids containing or likely to contain corrosive substance. When deadlegs are unavoidable, the length of the inactive pipe must be as short as possible to avoid stagnant or low-velocity flows.

Originality/value – The model solves the continuity and momentum equations for the mixture, and the volume fraction equation for the secondary phase utilizing an algebraic expression for the relative velocity.

Keywords Oils, Water, Fluid mechanics, Geometry, Flow measurement

Paper type Technical

Nomenclature

C = inlet concentration of water liquid
D_B, D = diameter of the branch
D_H = diameter of the header
L = length of the deadleg
V = inlet mixture velocity
C_μ = constant defined in equation (4)
C_1 = constant defined in equation (11)
C_2 = constant defined in equation (11)
G = generation of turbulent kinetic energy
g = gravitational acceleration
k = turbulent kinetic energy
p = pressure
$\overline{U_j}$ = average velocity component

The authors wish to acknowledge the support received from King Fahd University of Petroleum & Minerals during the course of this study.

International Journal for Numerical Methods in Heat & Fluid Flow
Vol. 15 No. 4, 2005
pp. 348-362

0961-5539
DOI 10.1108/09615530510590605

u_j = fluctuating velocity component
x_j = space coordinate

Greek letters
α = volume fraction
ε = dissipation rate of turbulent kinetic energy
μ = dynamic viscosity
ρ = density
σ = effective Prandtl number

Superscripts
– = time average

Subscripts
D = drift
eff = effective
ε = rate of dissipation of turbulent kinetic energy
f = fluid
k = kinetic energy of turbulence
m = mixture

1. Introduction

Deadleg is a term used to describe the inactive portion of a pipe, where the fluid is stagnant or has very low velocity, in various piping systems. In the petroleum and petrochemical industries, the deadlegs located in various piping systems represent weak spots because of the related corrosion problems. Deadlegs represent regions prone to corrosion in oil piping systems due to stagnant or low velocity flow that causes emulsified water precipitation out of the crude. In order to maintain the integrity of the connecting main pipe, internal corrosion of deadlegs must be prevented, since it is very difficult to control and usually requires a major shut down to fix. In the oil and gas industry, deadleg corrosion presents the highest percentage of internal damage to pipelines or in-plant piping systems that are normally considered to operate in a non-corrosive environment. Deadlegs should be avoided whenever possible in the design of piping for fluids containing or likely to contain corrosive substances. When deadlegs are unavoidable, the length of the inactive pipe must be as short as possible to avoid stagnant or low velocity flows.

To date, there is no research published on the effect of deadleg geometry and flow velocity on the concentration of water or other corrosive agents in deadlegs. Most of the relevant published work focused on the effect of oil to water ratio on the flow pattern and pressure drop in straight pipes. Amongst that published research is the work by Charles *et al.* (1961) who conducted an experimental investigation on the effect of oil-water ratio on the pressure gradient in a horizontal pipe. They found that at high oil-water ratio, oil formed the continuous phase and a water-drops-in-oil regime was observed. As the oil-water ratio was decreased, the flow patterns changed to concentric oil in water, oil-slugs-in-water, oil-bubbles-in-water and finally, oil-drops-in-water. The measured pressure gradient was found to strongly depend on the oil-water ratio. In another paper, Charles and Lilleleht (1966) presented the pressure gradient data obtained from three different sets of experiments for stratified flow of two immiscible liquids in laminar-turbulent regime using the parameters introduced by Lockhart and Martinelli (1949). The Lockhart and Martinelli parameters were used for correlating the pressure gradient data in case of gas-liquid mixture flows. Barnea (1986) presented unified models that incorporate the effect of the angle of inclination on the transition from annular flow to intermittent flow and from dispersed bubble flow. The models showed a smooth change in mechanisms as the pipe inclination varies over the whole range of upward and downward inclinations.

The stability of a stratified liquid-liquid two-phase system was investigated by Brauner and Maron (1992). They found that subzones of stratified-dispersed patterns

might appear in regions where stable stratification is expected. The reduction of density differential, as the case in liquid-liquid systems, tended to extend the regions of dispersed flow patterns on the account of the range of the continuous stratified patterns. The formation of a stratified-dispersed/stratified pattern was attributed to the moderate buoyancy forces in case of reduced density differential. Owing to the limited available experimental data, the model was not fully validated. Schmidt and Loth (1994) provided a practical and sufficiently accurate method for calculating the pressure drop in a tee junction with combining conduits using a semi-empirical approach. In their work, three basic models, termed the "loss coefficient model", "contraction coefficient model" and "momentum coefficient model" were derived. A formula based on comparison between the measured and the predicted pressure changes was recommended.

Plaxton (1995) conducted an experimental investigation on the effect of influx in a two-phase, liquid-liquid flow system on the pressure drop behavior. He found that the Brill and Beggs (1994) correlation method could provide adequate pressure gradient predictions for oil-water flow. On the other hand, the acceleration confluence model reported by Asheim *et al.* (1992) was found to be inadequate in predicting the pressure drops. Angeli and Hewitt (1996) reported their experimental results on the effect of the water volume fraction in an oil-water system on the pressure gradient in pipe flow. The water volume fraction ranged from 5 to 85 percent and the phase inversion point (the volume fraction of the dispersed phase above which this phase becomes continuous) appeared between 37 and 40 percent in both pipes. The pressure gradient measurements showed that the liquid-liquid dispersions exhibited a flow behavior that diverged from a single-phase flow. The measured values of the pressure gradient were much lower than those predicted from the homogeneous model. The experimental friction factors, especially in the oil continuous phase, appeared to be lower than the predictions of the homogeneous model. Similar studies for pressure losses in other pipefittings were carried out by Hwang and Pal (1997) for both sudden pipe expansion and sudden contraction and by Schabacker *et al.* (1998) for a sharp 180° bend.

An experimental study of oil-water flow patterns in horizontal pipes was conducted by Trallero *et al.* (1997) with emphasis on transition from one pattern to another. These flow patterns were classified into two main categories, namely segregated flow and dispersed flow. The segregated flow included two patterns, namely stratified flow pattern and stratified with some mixing at the interface while the dispersed flow included four patterns, two patterns were water dominated and the other two were oil dominated. A model was also proposed for predicting flow pattern transition for the case of using light oils. The model was based on a combination of the two-fluid model and the balance between gravity forces and turbulent fluctuations normal to the main flow. Other models were used for the stratified and dispersed flow patterns.

A new mathematical model for oil-water separation in pipes and tanks was proposed by Hafskjold *et al.* (1999). The model describes the process of water separation in oil systems based on the two mechanisms of coalescence and settling. The model was validated against experimental data and the comparison was satisfactory. The separation of oil and water can be considered as a combination of emulsification and separation. Hafskjold *et al.* (1999) observed that the separation rate for water in oil systems increases with the increase in water cut, and that some water

remains in the oil even after long settling times. These features may be qualitatively understood by a combination of coalescence and settling. Hafskjold *et al.* (1999) developed a mathematical-numerical model that describes these mechanisms qualitatively. This model calculates the quality of the output oil as function of system dimensions, flow rates, fluid physical properties, fluid quality, and drop size distribution at inlet.

After a comprehensive literature search, it was found that no research was published on the effect of deadleg length and orientation on water separation in deadleg regions that are widely used in oil piping systems. This study aims at investigating the effect of deadleg geometry and orientation on the velocity field and water separation in deadlegs. The present work also aims at establishing a deadleg criterion based on deadleg orientation and length to diameter ratio.

2. Problem statement

The problem considered is that of flow of an oil-water mixture having 90 percent oil and 10 percent water (by volume) in a tee junction with the deadleg forming one branch. The configuration considered for the deadleg is shown in Figure 1. The figure shows front, side, and plan views of the vertical deadleg. The calculations were carried out for various lengths of the deadleg where the length to diameter ratio $L/D_B = 1 - 7$ with the objective of obtaining the details of the flow velocity field as well as the changes in the water volumetric concentration inside the deadleg. This water concentration is important for corrosion prediction. The average inlet flow velocity is 1 m/s in all cases.

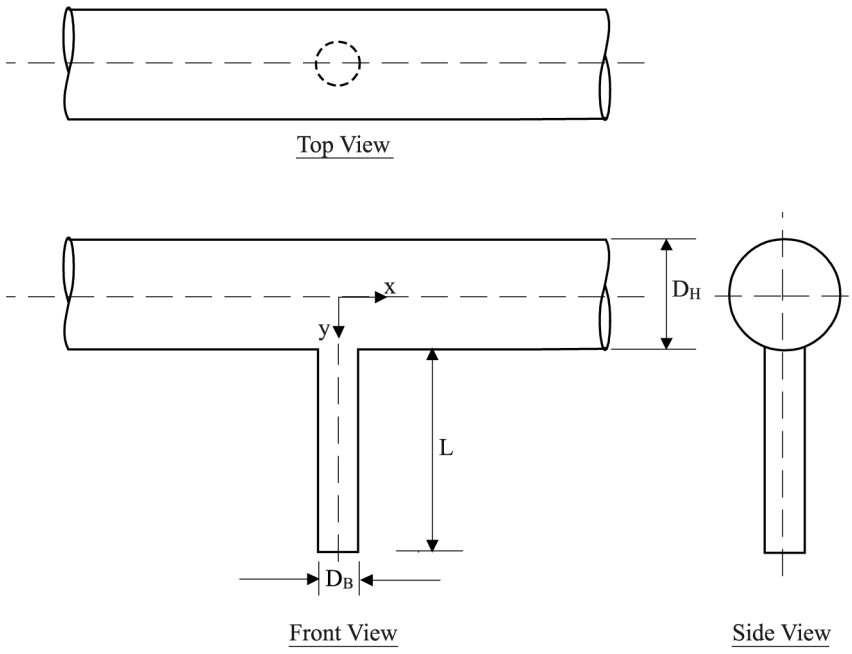

Figure 1.
The geometry of the deadleg configuratio

3. Mathematical formulation

The mathematical formulation for the calculation of the fluid flow field has been established. The fluid flow model is based on the time-averaged governing equations of 3D turbulent flow. The algebraic slip mixture model (Manninen *et al.*, 1996) is utilized for the calculation of the two immiscible fluids (water and crude oil). The model solves the continuity equation for the mixture, the momentum equation for the mixture, and the volume fraction equation for the secondary phase, as well as an algebraic expression for the relative velocity.

3.1 The continuity and momentum equations

Mass conservation. The steady-state time-averaged equation for conservation of mass of the mixture can be written as

$$\frac{\partial}{\partial x_j}(\rho \bar{U}_{\mathrm{m},j}) = 0 \tag{1}$$

Momentum conservation. The steady-state time-averaged equation for the conservation of momentum of the mixture in the i direction can be obtained by summing the individual momentum equations for both phases. It can be expressed as

$$\frac{\partial}{\partial x_j}(\rho \bar{U}_{\mathrm{m},i}\bar{U}_{\mathrm{m},j}) = -\frac{\partial p}{\partial x_i} + \frac{\partial}{\partial x_j}\left(\mu_{\mathrm{m}}\frac{\partial \bar{U}_{\mathrm{m},i}}{\partial x_j}\right) - \frac{\partial}{\partial x_j}(\rho\overline{u_{\mathrm{m},i}u_{\mathrm{m},j}}) + \rho_{\mathrm{m}}g + \sum_{k=1}^{2}\alpha_k\rho_k u_{\mathrm{D}k,i}u_{\mathrm{D}k,j} \tag{2}$$

where p is the static pressure and the stress tensor $\rho\overline{u_{\mathrm{m},i}u_{\mathrm{m},j}}$ is given by

$$-\rho\overline{u_{\mathrm{m},i}u_{\mathrm{m},j}} = \left[\mu_{\mathrm{eff}}\left(\frac{\partial \bar{U}_{\mathrm{m},i}}{\partial x_j} + \frac{\partial \bar{U}_{\mathrm{m},j}}{\partial x_j}\right)\right] - \frac{2}{3}\rho_{\mathrm{m}}k_{\mathrm{m}}\delta_{ij} \tag{3}$$

where δ_{ij} is the Kronecker delta which is equal to 1 for $i = j$ and equals 0 for $i \neq j$ and $\mu_{\mathrm{eff}} = \mu_{\mathrm{t}} + \mu$ is the effective viscosity. The turbulent viscosity, μ_{t}, is calculated using the high-Reynolds number form as

$$\mu_t = \rho_{\mathrm{m}}C_\mu\frac{k_{\mathrm{m}}^2}{\varepsilon_{\mathrm{m}}} \tag{4}$$

with $C_\mu = 0.0845$ (Versteeg and Malalasekera, 1995), k_{m} and ε_{m} are the kinetic energy of turbulence of the mixture and its dissipation rate. These are obtained by solving their conservation equations as given below.

ρ_{m} and μ_{m} in equation (2) are the density and viscosity of the mixture that can be obtained from

$$\rho_{\mathrm{m}} = \sum_{k=1}^{n}\alpha_k\rho_k. \tag{5}$$

$$\mu_m = \sum_{k=1}^{n} \alpha_k \mu_k. \tag{6}$$

$\bar{U}_{\mathrm{m}}$ is the mass-averaged velocity

$$\bar{U}_{\mathrm{m}} = \frac{\sum_{k=1}^{n} \alpha_k \rho_k \bar{U}_k}{\rho_m} \tag{7}$$

and $\bar{U}_{\mathrm{D}k}$ are the drift velocities.

$$\bar{U}_{\mathrm{D}k} = \bar{U}_k - \bar{U}_{\mathrm{m}}. \tag{8}$$

3.2 The volume fraction equation for the secondary phase

From the continuity equation for the secondary phase, the volume fraction equation for the secondary phase can be written as:

$$\frac{\partial}{\partial x_j}(\alpha_p \rho_p \bar{U}_{\mathrm{m},j}) = -\frac{\partial}{\partial x_j}(\alpha_p \rho_p \bar{U}_{p,j}). \tag{9}$$

3.3 Conservation equations for the turbulence model

The conservation equations of the turbulence model (Reynolds, 1987; Shih *et al.*, 1995) are given as follows.

The kinetic energy of turbulence:

$$\frac{\partial}{\partial x_j}(\rho \bar{U}_j k) = \frac{\partial}{\partial x_j}\left(\frac{\mu_{\mathrm{eff}}}{\sigma_k}\frac{\partial k}{\partial x_i}\right) + G_k - \rho\varepsilon. \tag{10}$$

The rate of dissipation of the kinetic energy of turbulence:

$$\frac{\partial}{\partial x_j}(\rho \bar{U}_j \varepsilon) = \frac{\partial}{\partial x_i}\left(\frac{\mu_{\mathrm{eff}}}{\sigma_\varepsilon}\frac{\partial \varepsilon}{\partial x_i}\right) + C_1 G_k \frac{\varepsilon}{k} - C_2 \rho \frac{\varepsilon^2}{k} \tag{11}$$

where G_{k} represents the generation of turbulent kinetic energy due to the mean velocity gradients and is given by

$$G_k = -\rho \overline{u_i u_j} \frac{\partial \bar{U}_j}{\partial x_i} \tag{12}$$

The quantities σ_k and σ_ε are the effective Prandtl numbers for k and ε, respectively, and C_2 is given by Shih *et al.* (1995) as a function of the term k/ε and, therefore, the model is responsive to the effects of rapid strain and streamline curvature and is suitable for the present calculations. The model constants C_1 and C_2 have the values; $C_1 = 1.42$ and $C_2 = 1.68$.

The wall functions establish the link between the field variables at the near-wall cells and the corresponding quantities at the wall. These are based on the assumptions introduced by Launder and Spalding (1974) and have been most widely used for industrial flow modeling. The details of the wall functions are provided by the law-of-the-wall for the mean velocity as given by Habib *et al.* (1989).

3.4 Boundary conditions

The velocity distribution is considered uniform at the inlet section kinetic energy and its dissipation rate are assigned through a specified value of $\sqrt{k/\bar{U}^2}$ equal to 0.1 and a length scale, L, equal to the diameter of the inlet section. The boundary condition applied at the exit section (outlet of the heat exchanger tubes) is that of fully developed flow. At the wall boundaries, all velocity components are set to zero in accordance with the no-slip. Kinetic energy of turbulence and its dissipation rate are determined from the equations of the turbulence model. The secondary-phase volume fraction is specified at the inlet and exit sections of the flow domain.

3.5 Solution procedure

The calculations were obtained using the Fluent CFD-5.5 package. The conservation equations are integrated over a typical volume that is formed by division of the flow field into a number of control volumes to yield the solution. The equations are solved simultaneously using the solution procedure described by Patankar (1980). Calculations are performed with at least 300,000 volumes. Convergence is considered when the maximum of the summation of the residuals of all the elements for U, V, W and pressure correction equations is less than 0.1 percent. The grid independence tests were performed by increasing the number of control volumes from 260,000 to 380,000 in two steps. Figure 2(a) shows the effect of mesh refinement on the velocity variation along the axis of the deadleg. The effect of mesh refinement on the volumetric water concentration along the same axis is shown in Figure 2(b). The influence of refining the grid on the velocity is very negligible. The grid independence test resulted in a maximum difference of less than 2.5 percent in the volumetric water concentration as the number of finite volumes increased from 260,000 to 320,000 and less than 0.8 percent as the number of finite volumes further increased from 320,000 to 380,000. The above-mentioned figures and percentage differences indicate that more mesh refinement will result in negligible changes in the accuracy of the computational model.

4. Results and discussion

The details of the flow velocity field were obtained for steady-state conditions at different deadleg geometries (different deadleg lengths). The fluid at the inlet section in

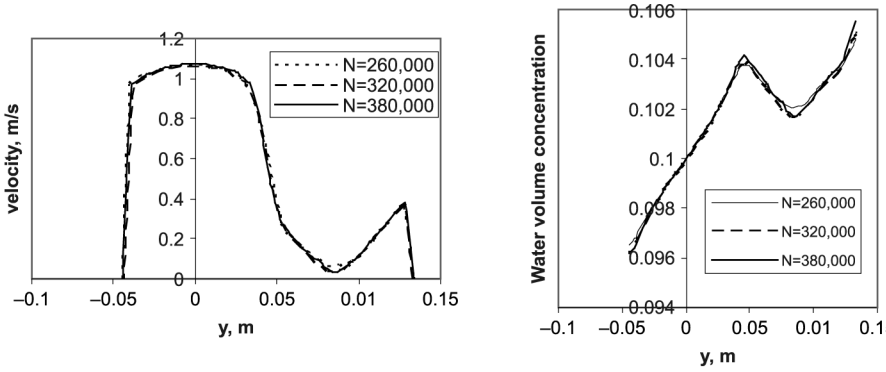

(a) Velocity magnitude

(b) Volumetric water concentration

Figure 2.
The influence of mesh refinement on the velocity magnitude and volumetric water concentration along the axis of the deadleg, L/D_B1

all of the considered cases is a homogeneous mixture containing 90 percent crude oil, by volume, and 10 percent water and the average flow velocity at inlet is 1 m/s. The header and branch diameters are D_H=0.3 and D_B=0.1 m for all cases. The vertical deadleg has four values of the length to diameter ratios ($L/D_B = 1, 3, 5$, and 7). The influence of L/D_B ratio on the velocity vectors and contours of the volumetric water concentration is presented. Figure 3 shows the contours of velocity vectors for the case of $L/D_B = 1$. In this case, the core region of the main pipe has almost uniform velocity distribution with large velocity gradient near the wall as what one would expect in the case of fully developed turbulent flow in a pipe. The velocity is high at the top, bottom, and side regions of the deadleg while low velocity exists at the middle. This distribution indicates the existence of a circulating flow zone similar to that occurring in a rectangular cavity with an upper moving boundary (Chiang *et al.*, 1998). It is clear from the figure that a circulating flow zone exists in the deadleg that acts as a cylindrical cavity with its upper boundary open to the main stream. Such circulating flow pattern tends to eliminate the stagnant fluid zone in the vertical deadleg. The present calculations are validated by comparison with the results of flow visualization as shown in Figure 3. The comparison is made for $L/D_B = 1.0$. The flow pattern of the calculated results is in good agreement with the flow visualization results.

Figure 4 shows the contours of velocity vectors for different cases of L/D_B. Figure 4(b) shows the velocity vectors in the case of $L/D_B = 3$. It is clear from these figures that the circulating flow zone extends over most of the entire length of the deadleg, however, with low velocity in the lower portion (about 0.05 m/s). The velocity vectors for $L/D_B > 3$ are shown in Figures 4(c) and (d). Similar to the case of $L/D_B = 1$, a circulating flow region occurs in the upper part of the deadleg. The length of this part is equal to 2.3*D*. A stagnant fluid zone appears in the middle and lower portions of the deadleg in cases of $L/D_B > 3$ as shown in Figure 4(c) and (d). Figure 4(c) shows a stagnant fluid region appearing near the wall in the case of $L/D_B = 5$. That region extends, in a scattered fashion, in the lower part of the deadleg. The size of that region is found to increase with increasing L/D_B. Figure 4(d) shows an interesting flow pattern

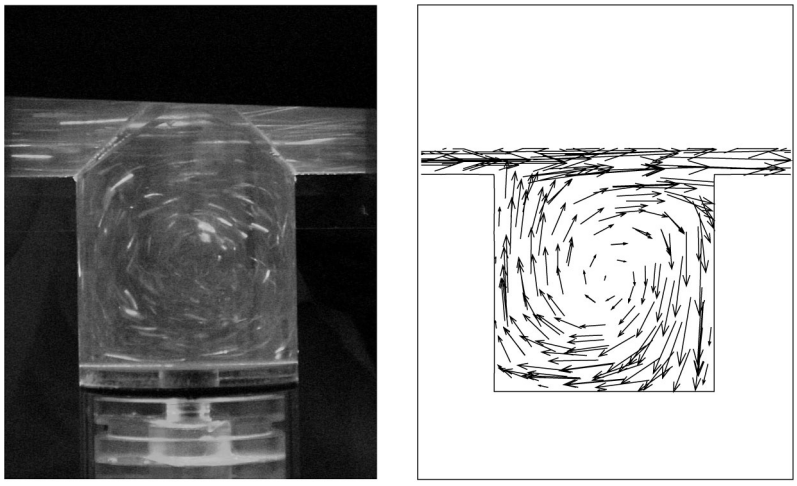

Figure 3.
Calculated and measured velocity vectors inside the deadleg of L/D_B=1

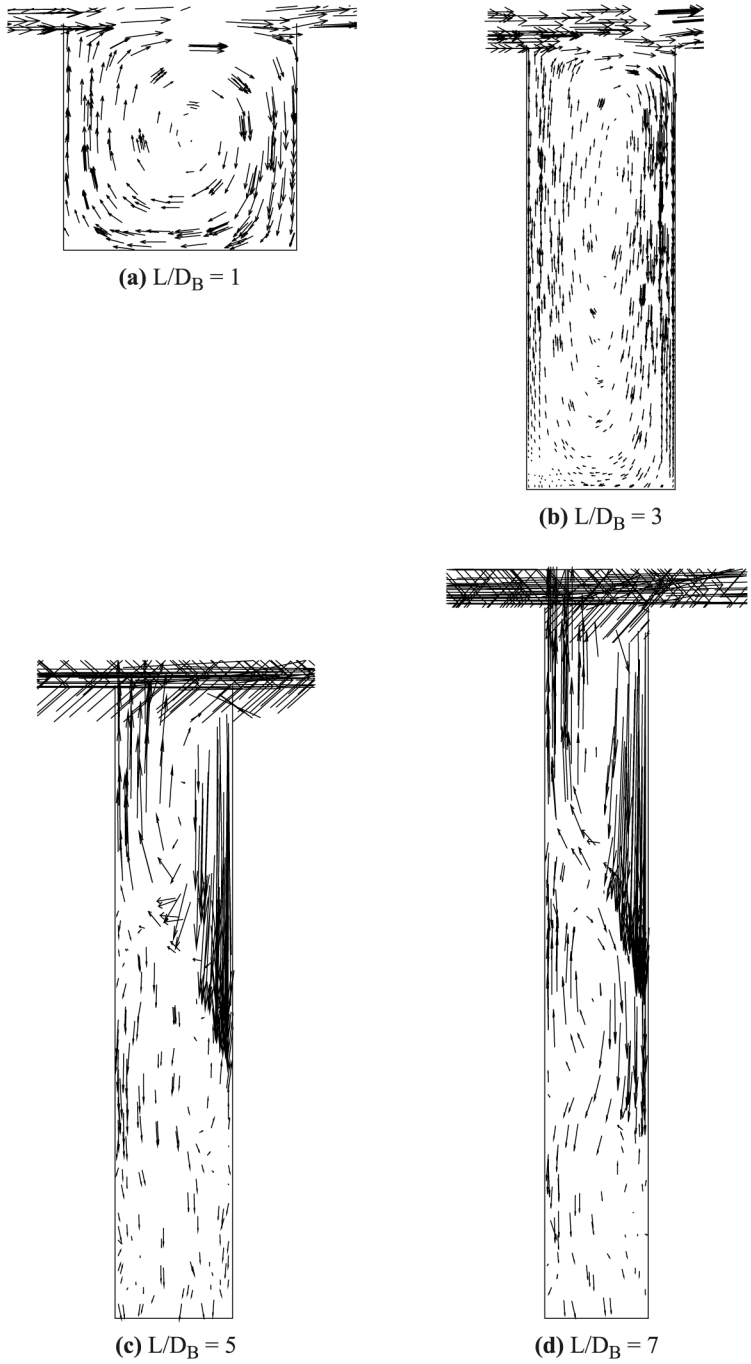

(a) $L/D_B = 1$

(b) $L/D_B = 3$

(c) $L/D_B = 5$

(d) $L/D_B = 7$

Figure 4.
Influence of the deadleg length on the velocity vectors

in which the upper section of the deadleg ($0 < y < 2.8D_B$) is characterized by a circulating flow zone similar to that found in the case of $L/D_B = 3$. This is followed by the middle section ($2.8D < y < 5.2D_B$) that is occupied by several counter-rotating vortices. The lower section ($5.2D < y < 7D_B$) is occupied by a stagnant fluid. The total length of the deadleg occupied by a stagnant fluid is $4.2D$ that corresponds to 60 percent of the deadleg length. Considering the fact that the vortices in the middle region are too weak with negligible velocity magnitudes, it can be concluded that almost 70 percent of the deadleg is occupied by stagnant fluid.

Figure 5 shows the influence of the deadleg length to diameter ratio on the local water concentration in the vertical deadleg. The effect of deadleg length on the variation of local water concentration in the vertical deadleg is shown in Figure 5(a) for the case of $L/D_B = 1$. The local water concentration is found to be slightly higher than 10 percent (ranging between 10.2 and 10.4 percent) with the maximum concentration at the top and bottom regions of the deadleg. Having this maximum water concentration at the bottom is quite expected because of gravity effects, but having the same value at the top may create some confusion. Actually, the maximum water concentration should occur at the bottom of the deadleg in the case of a stagnant fluid, however, because of the strong vortical motion (see Figure 4(a)), the same concentration reaches the top region. Figure 5(b) shows the contours of the water volumetric percentage for the case of $L/D_B = 3$. The figure shows that the water concentration varies from 10.2 to 11.7 percent with the maximum occurring in a very small region at the bottom of the deadleg. The slight increase in the water concentration close to the deadleg bottom (in comparison with the case of $L/D_B = 1$) is due to the small stagnant region in the vicinity of the deadleg bottom.

Increasing L/D_B from 3 to 5 is found to create very high values of water concentration that reaches 86.7 percent at the bottom region as shown in Figure 5(c). In this case, the upper half of the deadleg has a water concentration in the range from 14 to 39 percent while the lower half has a concentration in the range from 40 to 86.7 percent with maximum value at the bottom of the deadleg. The part of the deadleg that has high water concentration of more than 20 percent is about 46 percent of the deadleg length (about $2.3D_B$). The situation is almost the same in the case of $L/D_B = 7$ (see Figure 5(d)), however, the region of high water concentration (more than 20 percent) occupies about 40 percent of the deadleg length (about $2.8D_B$). Table I shows the range of local water concentration in the deadleg for different values of length-to-diameter ratios. Thus, for the vertical deadleg, it is clear that there is no stagnant fluid zone in all cases so long as $L/D_B < 3$. For the cases of $L/D_B > 3$, it is also clear that the region of the deadleg close to the header is characterized by circulating vortical motions for a length $l \approx 3D_B$ while the remaining part of the deadleg occupied by stagnant fluid.

The vertical component of the mean velocity is presented along the radial (x-direction) in Figures 6-9 for the different cases of L/D_B. The case for $L/D_B = 1$ is shown in Figure 6. As can be seen from the figure, the profile at $y = 0.5D$ shows that the flow moves upward at a velocity reaching a maximum of 0.4 m/s in the region of positive x and moves downward with a minimum value of -0.32 m/s in the region of negative x. For the case of $L/D_B = 3$, the same phenomenon shown for $L/D_B = 1$ appears for all profiles, with the vortex getting weaker as y increases and at $y/D_B = 2.5$ in particular. In this case, the maximum value is 0.15 m/s and the minimum value is 0.08 m/s. Figures 8 and 9 show the velocity profiles for the case of $L/D_B = 5$ and 7 and

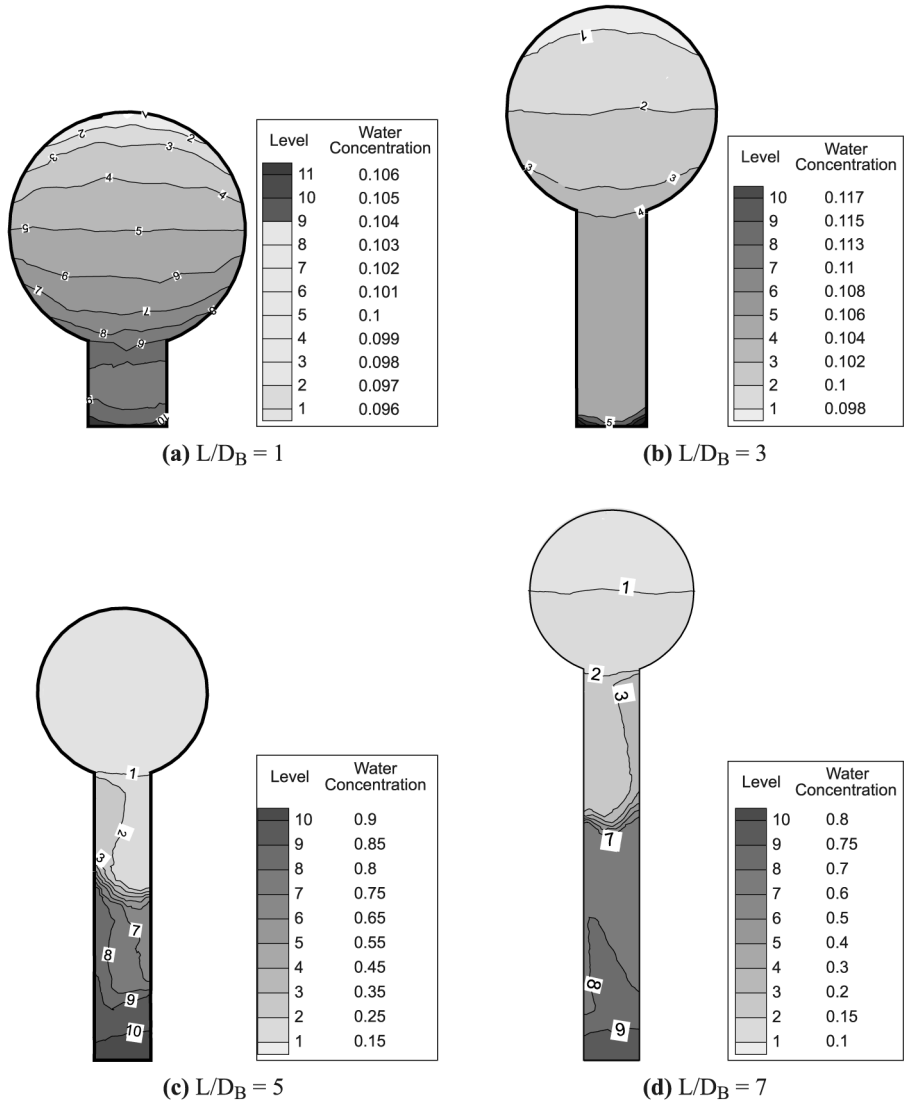

Figure 5.
Influence of the deadleg length on the contours of the volumetric concentration of water

Table I.
Range of local water concentration in a deadleg with D_H=0.3, D_B=0.1 m and V = 1 m/s for different length-to-diameter ratios

L/D_B	Range of water concentration (percent)	Length of regions with circulating flow	Length of region(s) with water concentration ≤20 percent
1	10.2-10.4	None	None
3	10.2-11.7	2.8 D_B	2.9-3 D_B
5	14.0-86.7	2.3 D_B	2.1 D_B
7	13.2-82.2	2.8 D_B	2.6 D_B

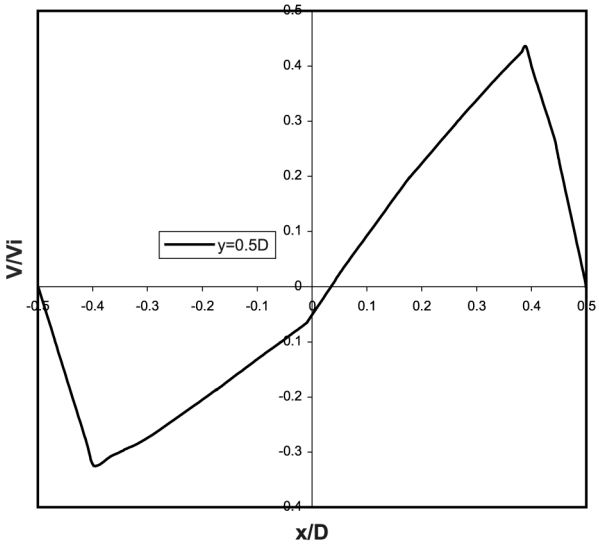

Figure 6.
The velocity across the vertical deadleg section; $L/D_B=1$

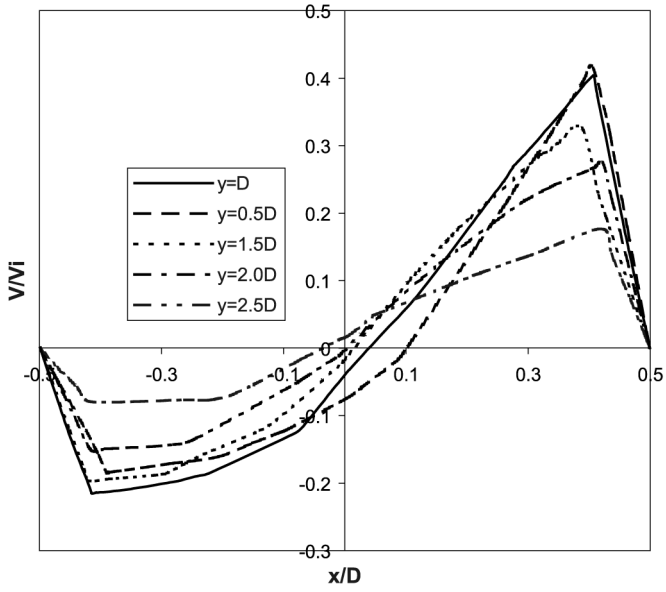

Figure 7.
The velocity across the vertical deadleg section; $L/D_B=3$

indicate that the vortex become very weak with maximum and minimum values of less than 0.05 m/s for $y/D_B > 2.5$.

In order to show the influence of L/D_B on the oil/water separation, the volumetric water concentration along the axis of the vertical deadleg for different deadleg lengths is shown in Figure 10. The figure indicates that insignificant changes of water concentrations are shown for L/D_B=1-3 along the y direction. This is not the case for

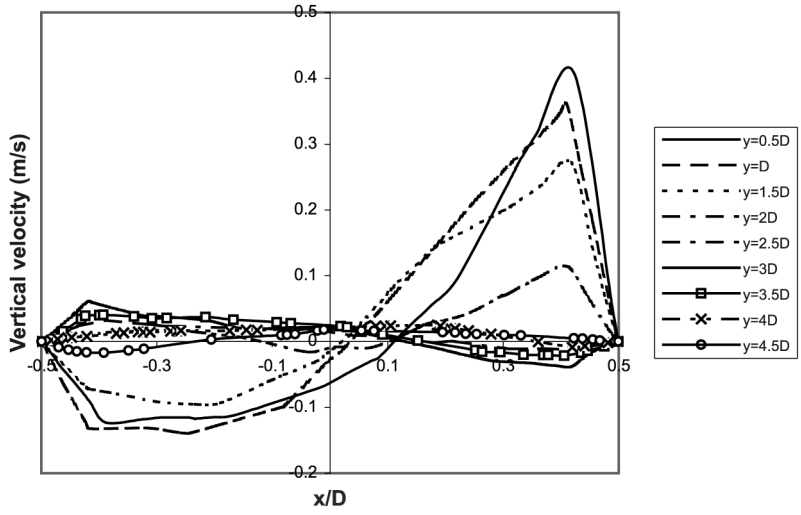

Figure 8.
The velocity across the vertical deadleg section; $L/D_B=5$

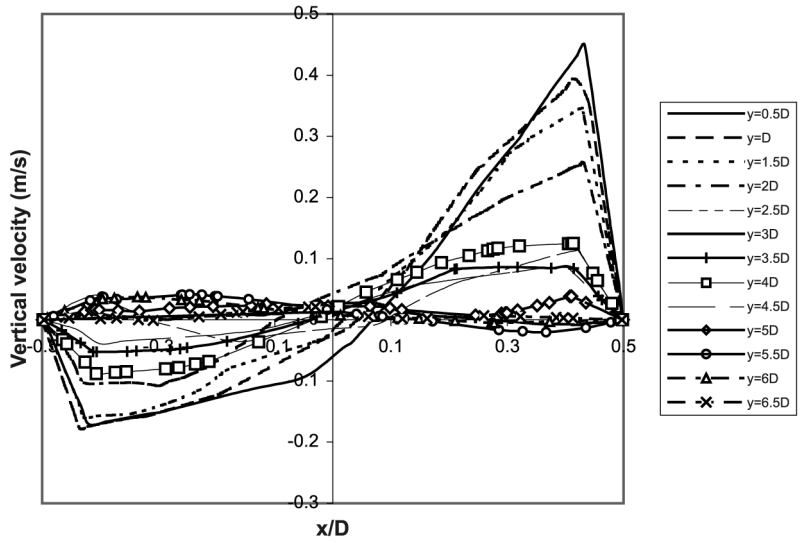

Figure 9.
The velocity across the vertical deadleg section; $L/D_B=7$

L/D_B equal to 5 or 7. In these two cases, the water concentration increases to approximately 15-25 percent in the vicinity of the center of the tube and remains almost constant up to $L/D_B=1.5$-3 and then increases sharply to 0.7. Following this, a gradual increase is shown till the end of the deadleg, where the water concentration reaches 80 percent. These results confirm those of Figures 4 and 5 that the deadleg can be defined for regions of the deadleg length of more than $\sim 3D_B$.

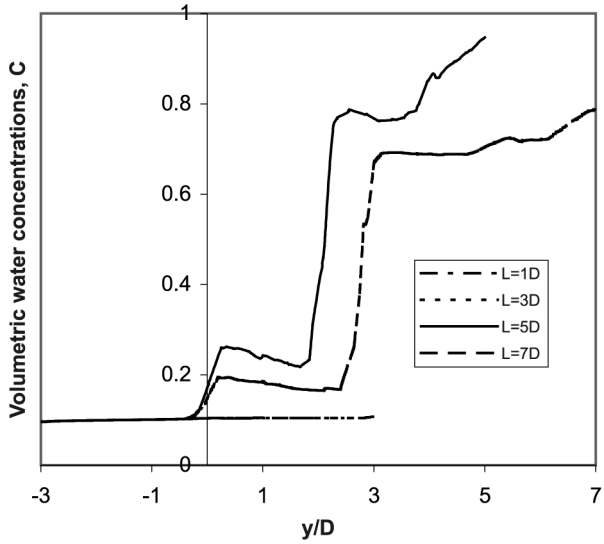

Figure 10.
The volumetric water concentration across the vertical deadleg section for different deadleg lengths

5. Conclusions

The effect of deadleg geometry on flow field and oil/water separation was investigated. The investigation is based on the solution of the mass and momentum conservation equations of an oil/water mixture together with the volume fraction equation for the secondary phase. A fluid flow model based on the time-averaged governing equations of 3D turbulent flow has been developed. An algebraic slip mixture model is utilized for the calculation of the two immiscible fluids (water and crude oil). Results are obtained for length to diameter ratios ranging from 1 to 7. The considered fluid mixture contains 90 percent oil and 10 percent water (by volume) and the inlet flow velocity is kept constant (1 m/s). The results show that the size of the stagnant fluid region increases with the increase of L/D_B. It is found that the region of the deadleg close to the header is characterized by circulating vortical motions for a length $l \approx 3D_B$ while the remaining part of the deadleg occupied by a stagnant fluid. The results also indicated that the water volumetric concentration increases with the increase of L/D_B and influenced by the deadleg orientation. Maximum value of the water concentration increases from 10.4 percent in the case of $L/D_B=1$ to more than 80 percent in the case of $L/D_B=7$ for the vertical deadleg.

References

Angeli, P. and Hewitt, G.F. (1996), "Pressure gradient phenomena during horizontal oil-water flow", 1996 OMAE – Volume V, ASME 1996, *Pipeline Technology*, pp. 287-95.

Asheim, H., Kolnes, J. and Oudeman, P. (1992), "A flow resistance correlation for completed wellbore", *Journal of Petroleum Science & Engineering*, Vol. 8 No. 2, pp. 97-104.

Barnea, D. (1986), "Transition from annular flow and from dispersed bubble flow-unified models for the whole range of pipe inclinations", *International Journal of Multiphase Phase Flow*, Vol. 12 No. 5, pp. 733-44.

Brauner, N. and Maron, D.M. (1992), "Stability analysis of stratified liquid-liquid flow", *International Journal of Multiphase Flow*, Vol. 18 No. 1, pp. 103-21.

Brill, J. and Beggs, H. (1994), *Two-Phase Flow in Pipes*, 6th ed., University of Tulsa Press, Tulsa, OK.

Chiang, T.P., Sheu, W.H. and Hwang, R.R. (1998), "Effect of Reynolds number on the eddy structure in a lid-driven cavity", *International Journal of Numerical Methods in Fluids*, Vol. 26, pp. 557-79.

Charles, M.E. and Lilleleht, L.U. (1966), "Correlations of pressure gradients for the stratified laminar-turbulent pipeline flow of two immiscible liquids", *The Canadian Journal of Chemical Engineering*, pp. 47-9.

Charles, M.E., Govier, G.W. and Hodgson, G.W. (1961), "The horizontal pipeline flow of equal density oil-water mixture", *The Canadian Journal of Chemical Engineering*, pp. 27-36.

Habib, M.A., Attya, A.M. and McEligot, D.M. (1989), "Calculation of turbulent flow and heat transfer in channels with streamwise periodic flow", *ASME Journal of Turbomachinery*, Vol. 110, pp. 405-11.

Hafskjold, B., Celius, H.K. and Aamo, O.M. (1999), "A new mathematical model for oil/water separation in pipes and tanks", *SPE Production and Facilities*, Vol. 14 No. 1, pp. 30-6.

Hwang, C.J. and Pal, R. (1997), "Flow of two-phase oil/water mixtures through sudden expansions and contractions", *Chemical Engineering Journal*, Vol. 68, pp. 157-63.

Launder, B.E. and Spalding, D.B. (1974), "The numerical computation of turbulent flows", *Computer Methods in Applied Mechanics and Engineering*, Vol. 3, pp. 269-89.

Lockhart, R.W. and Martinelli, R.C. (1949), "Proposed correlation of data for isothermal two-phase, two-component flow in pipes", *Chemical Engineering Progress*, Vol. 45, pp. 39-48.

Manninen, M., Taivassalo, V. and Kallio, S. (1996), *On the Mixture Model for Multiphase Flow*, Technical Research Center of Finland, VIT Publications.

Patankar, S.V. (1980), *Numerical Heat Transfer and Fluid Flow*, 1st ed., Taylor and Francis, Chichester, New York, NY.

Plaxton, B.L. (1995), "Pipeflow experiments for analysis of pressure drop in horizontal wells", paper presented at the SPE Annual Technical Conference and Exhibition, Dallas, TX, October 22-25, pp. 635-50.

Reynolds, W.C. (1987), "Fundamentals of turbulence for turbulence modeling and simulation", Lecture Notes for Von Karman Institute, Agard Report No. 755.

Schabacker, J., Bolcs, A. and Johnson, B.V. (1998), "PIV investigation of the flow characteristics in an internal coolant passage with two ducts connected by a sharp 180° bend", paper presented at the Int. Gat Turbine & Aeroengine Congress and Exhibition, Fairfield, NJ, 2-5 June, paper 98-GT-544.

Schmidt, H. and Loth, R. (1994), "Predictive methods for two-phase flow pressure loss in tee junctions with combining ducts", *International Journal of Multiphase Flow*, Vol. 20 No. 4, pp. 703-20.

Shih, T.H., Liou, W.W., Shabbir, A. and Zhu, J. (1995), "A new k-ε eddy-viscosity model for high Reynolds number turbulent flows – model development and validation", *Computers and Fluids*, Vol. 24 No. 3, pp. 227-38.

Trallero, J.L., Sarica, C. and Brill, J.P. (1997), "A study of oil/water flow patterns in horizontal pipes", *SPE Production and Facilities*, August, pp. 165-72.

Versteeg, H.K. and Malalasekera, W. (1995), *An Introduction to Computational Fluid Dynamics; The Finite Volume Method*, Longman Scientific and Technical, New York, NY.